






Article

Synthesis and Characterization of Calcium Carbonate Obtained from Green Mussel and Crab Shells as a Biomaterials Candidate

Rifky Ismail ^{1,*}, Tezara Cionita ^{2,*}, Wong Ling Shing ³, Deni Fajar Fitriyana ⁴ , Januar Parlaungan Siregar ⁵ , Athanasius Priharyoto Bayuseno ¹, Fariz Wisda Nugraha ¹ , Rilo Chandra Muhamadin ¹, Ramli Junid ⁵ , and Nor Azam Endot ⁶ 

¹ Department of Mechanical Engineering, Faculty of Engineering, Diponegoro University, Semarang 50275, Indonesia

² Faculty of Engineering and Quantity Surveying, INTI International University, Nilai 71800, Malaysia

³ Faculty of Health and Life Sciences, INTI International University, Nilai 71800, Malaysia

⁴ Department of Mechanical Engineering, Universitas Negeri Semarang, Kampus Sekaran, Gunungpati, Semarang 50229, Indonesia

⁵ College of Engineering, Universiti Malaysia Pahang, Gambang 26300, Malaysia

⁶ Department of Chemistry, Faculty of Science, Universiti Putra Malaysia, Serdang 43400, Malaysia

* Correspondence: r.ismail.undip@gmail.com (R.I.); tezara.cionita@newinti.edu.my (T.C.)

Abstract: Green mussel and crab shells are natural sources of CaCO_3 , which is widely used as a bioceramic for biomedical applications, although they are commonly disposed of in landfills. The improper disposal of green mussel and crab shells can cause environmental pollution, reducing the quality of life in the community. Many studies have reported the preparation of CaCO_3 from green mussels and crab shells. However, there are limited studies comparing the characteristics, including the crystal phase obtained, weight percentage (%) of crystal, crystal size, crystal system, and elemental composition of CaCO_3 from green mussel shells, crab shells, and commercial CaCO_3 . The objective of this research was to compare the calcium carbonate properties formed from green mussel (PMS) and crab (PCS) shells to commercial CaCO_3 . Green mussel and crab shells were crushed to powder and were calcined at 900 °C for 5 h. Precipitated Calcium Carbonate (PCC) was synthesized from calcined green mussel and crab shells using a solution of 2M HNO_3 , NH_4OH , and CO_2 gas. The effect of setting parameters on the synthesized product was analyzed using XRD and SEM-EDX methods. This study shows that the chemical composition of PMS is nearly identical to that of commercial CaCO_3 , where no contaminants were identified. In contrast, PCS has N components other than Ca, C, and O. Furthermore, the predominance of the vaterite crystal phases in PMS and PCS, with respective weight percentages of 91.2% and 98.9%, provides a benefit for biomaterial applications. The crystallite sizes of vaterite in PMS, PCS, and calcite in commercial CaCO_3 are 34 nm, 21 nm, and 15 nm, respectively.

Keywords: mussel and crab shells; precipitation; calcium carbonate; bioceramic; biomedical



Citation: Ismail, R.; Cionita, T.; Shing, W.L.; Fitriyana, D.F.; Siregar, J.P.; Bayuseno, A.P.; Nugraha, F.W.; Muhamadin, R.C.; Junid, R.; Endot, N.A. Synthesis and Characterization of Calcium Carbonate Obtained from Green Mussel and Crab Shells as a Biomaterials Candidate. *Materials* **2022**, *15*, 5712. <https://doi.org/10.3390/ma15165712>

Academic Editor: Bongju Kim

Received: 20 July 2022

Accepted: 8 August 2022

Published: 19 August 2022

Publisher's Note: MDPI stays neutral with regard to jurisdictional claims in published maps and institutional affiliations.



Copyright: © 2022 by the authors. Licensee MDPI, Basel, Switzerland. This article is an open access article distributed under the terms and conditions of the Creative Commons Attribution (CC BY) license (<https://creativecommons.org/licenses/by/4.0/>).

1. Introduction

Shellfish are animals that live in water (salt water or fresh water) and have a shell or shell-resembling exterior. Commonly, shellfish can be divided into crustaceans and mollusks [1]. Crustaceans are aquatic animals that have jointed legs, a hard shell, and no backbone, such as crabs, crayfish, lobsters, prawns, and shrimp. Most mollusks have a hinged two-part shell, including clams, green mussels, oysters, and scallops, and various octopuses, snails, and squids. Shellfish has been a popular and favorite food in ancient and modern civilizations.

This has occurred because fresh shellfish is an excellent source of protein and a good source of minerals for humans. Additionally, most shellfishes are low in fat, cholesterol, and sodium [1].

Green mussels and crabs are examples of shellfishes widely consumed and traded by Indonesians, such as in Central Java. In 2019, the production of green mussels and crab in Central Java reached 12,500 tons [2] and 161 tons [3], respectively, to meet domestic and export needs. The green mussel shells and crab shells represent 70% [4] and 50% [5] of the total production, so the Province of Central Java produced 8750 tons of green mussel shells and 80.5 tons of crab shells in 2019. The results of these calculations show that the waste of green mussels and crab is very abundant and easy to find in the province of Central Java.

The improper disposal of solid waste in the form of green mussel shells and crab shells can cause environmental pollution, reducing the quality of life of the community. Green mussel and crab shells, including seashells, are very rich in calcium carbonate [4]. Nanoparticles such as calcium carbonate found in seashells are the main target of researchers' applications in the biomedical field [6]. Currently, the main production of calcium carbonate comes from geological sources, with market prices varying from USD 60 per ton for coarse particles to USD 250 per ton for fine particles. However, calcium carbonate from geological sources has the risk of containing heavy metals, which are harmful to humans. Meanwhile, calcium carbonate from seashells such as green mussel and crab shells is relatively safe for human consumption and medical applications. The market price of medical-grade calcium carbonate can be as high as USD 1600 per ton [7].

PCC stands for Precipitated Calcium Carbonate, also known as purified, refined, or synthetic calcium carbonate. In general, PCC is when calcium carbonate is hydrated and then reacted with carbon dioxide. PCC has a high economic value because it has advantages such as size distribution, crystal phase, and specific surface area, which can be controlled during the synthesis process. Due to its excellence, PCC is widely applied in the pharmaceutical, biological, and biomedical fields [8]. Calcium carbonate from seashells such as green mussel and crab shells as a raw material for bioceramics for biomedical applications provides economic and environmental benefits. Economic advantages are due to the low price of waste, the availability in large quantities, and the ease of obtainment. Meanwhile, the use of waste materials directly can reduce environmental problems [9]. Bioceramics of seashells in biomedical applications are used for bone graft substitutes [10–12], dental materials [5,13,14], and drug delivery systems [6,15–17]. Calcium phosphate (CaP) bioceramics such as hydroxyapatite (HA) and tricalcium phosphate (TCP) are used for bone substitutes because they have excellent biocompatibility and osteoconductive properties [18]. Therefore, the objective of the present study is to compare the physical properties of commercial calcium carbonate and calcium carbonate synthesized from green mussel and crab shells that are easily found in the Central Java Province, Indonesia.

2. Materials and Methods

The green mussel and crab shells in this study were obtained from the province of Central Java, Indonesia. After cleaning, the green mussel and crab shells were oven-dried at 100 °C for 2 h. The dried green mussel and crab shells were reduced using a crusher machine and sieved with 100 mesh screens. This process produced the green mussel and crab shell powders. The calcination process was carried out on the green mussel and crab shell powders using a Thermolyne Furnace Chamber F6010 at a temperature of 900 °C for 5 h. The green mussel and crab shell powders before and after calcination were characterized using SEM-EDX and XRD methods.

In this study, Precipitated Calcium Carbonate (PCC) was synthesized using calcined green mussel and crab shell powders. Seventeen grams of calcined crab shell powder were mixed with 300 mL of 2M HNO₃.

To produce a homogeneous mixture, stirring was carried out using a magnetic stirrer at 60 °C for 30 min with a rotation speed of 30 rpm. After 30 min, NH₄OH was added until the pH of the solution reached 12, which was then filtered using Whatman 42 filter paper. The filtrate was precipitated by slowly flowing CO₂ gas. The resulting milky white precipitate was then washed and filtered with distilled water to a pH of 7 and then dried at

110 °C for 2 h. The exact process was also carried out to produce PCC made from calcined green mussel shell powder [19].

SEM-EDX (SEOL JSM–6510LA) method was used to determine PCC's morphology and chemical elements made of green mussel and crab shells. The Shimadzu XRD-7000 was also used to analyze PCC's resulting phase and crystallite size from the green mussel and crab shells. Crystalline phases presented in the samples were identified with the help of the Joint Committee on Powder Diffraction Standards (JCPDS). The Rietveld analysis was conducted using the High Score Plus software version 3.0e from PANalytical X'Pert, Cambridge, UK. The description of the diffraction line profiles at Rietveld refinement was achieved using the pseudo-Voigt function. For comparison, SEM-EDX dan XRD tests were held to commercial-grade calcium carbonate gained from Merck.

3. Results and Discussion

3.1. Characterization of Green Mussel and Crab Shell Powders

Figure 1 shows a graphic comparison of the XRD test results on green mussel and crab shell powder. Calcite and aragonite crystalline phases were found in powdered green mussel and crab shells. Following JCPDS card number 05-0586, the phase of calcite crystals in mussel and crab shell powder is generally denoted as 2θ : 29.404, 39.399, and 43.143. Meanwhile, the aragonite crystal phase is shown at 2θ : 26.312, 31.176, and 33.180 (JCPDS Card No. 05-0453). In this study, the powder of green mussel shells was dominated by an aragonite crystal phase with a little calcite crystal phase. This contrasts with the crystalline phase found in powdered crab shells dominated by the calcite crystalline phase with a little aragonite crystalline phase.

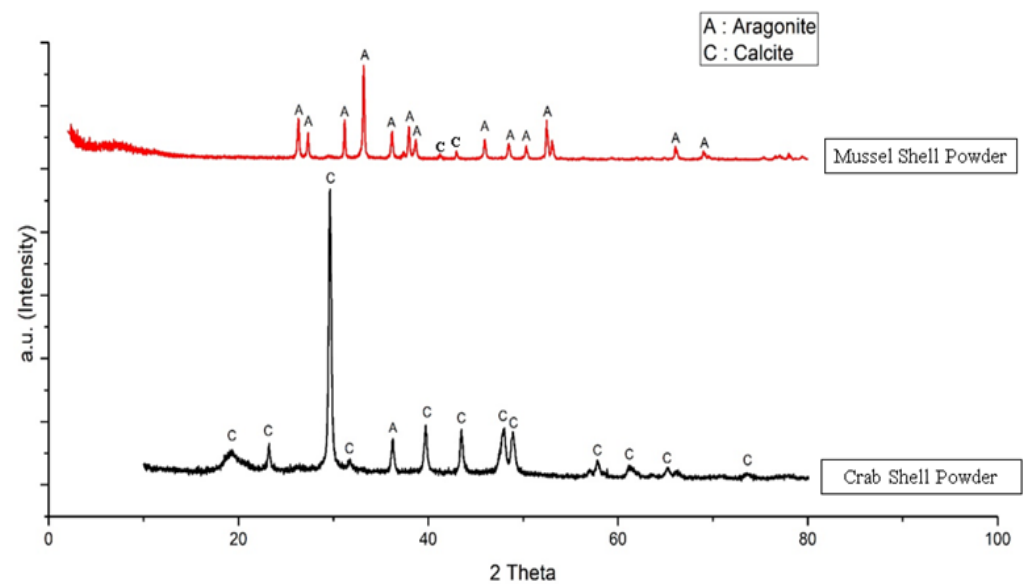


Figure 1. XRD diffraction pattern of green mussel and crab shell powders.

The comparison of the weight percentage (%) phase of calcite and aragonite crystals on green mussel and crab shell powders is shown in Figure 2. Weight percentage (%) of calcite and aragonite crystals were generated from a Rietveld analysis carried out using High Score Plus software version 3.0e, as shown in Figure 3a,b. In the green mussel shells powder, the aragonite crystal had a weight percentage (%) and crystallite size of 98.6% and 59 nm, respectively, with an orthorhombic crystal system. Meanwhile, the calcite phase in the crab shells powder showed a trigonal crystal system with a weight percentage (%) and crystallite size of 91.8% and 19 nm.

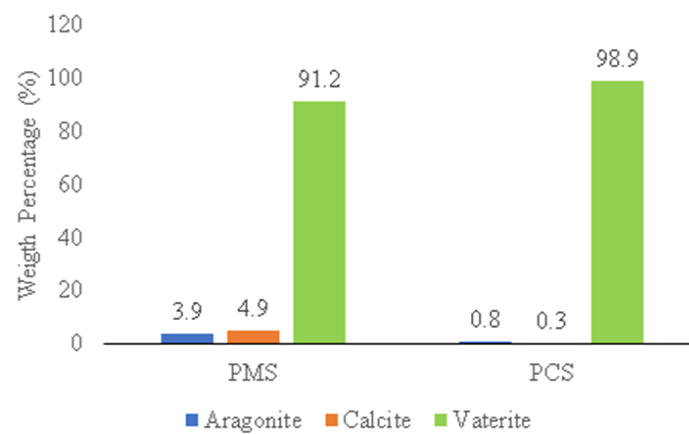
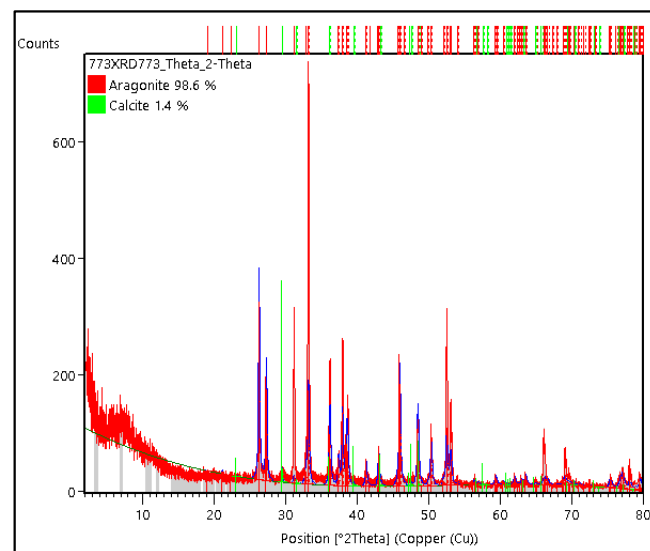
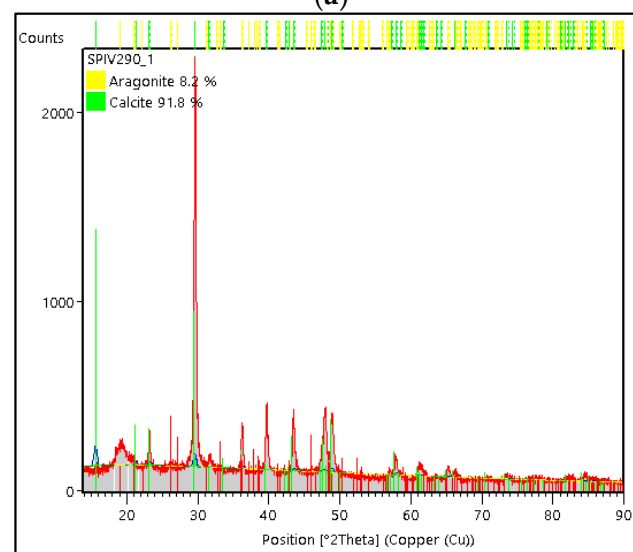


Figure 2. Comparison of weight percentage (%) of crystal phase on green mussel shell and crab shell powder.



(a)



(b)

Figure 3. XRD diffraction patterns of (a) green mussel shells powder and (b) crab shell powder.

The XRD test results on green mussel and crab shell powders showed the crystal phase of aragonite and calcite dominance, respectively. This is supported by the SEM test results shown in Figure 4a,b. Scanning Electron Microscopy (SEM) was used to study the morphology of the synthesis product [20–22]. The morphology of the green mussel shell powder is irregular in shape and resembles a small branching rod, which represents the characteristics of aragonite crystals [23]. The common morphologies of aragonite are rod-like, multilayered, pseudo-hexagonal, needle-like, and dendrite-like [24].

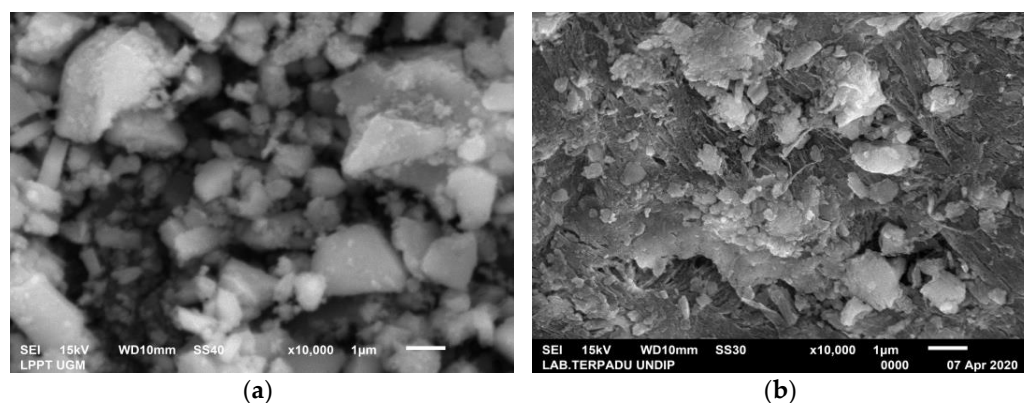


Figure 4. SEM images of (a) green mussel shells powder and (b) crab shell powder.

Meanwhile, the morphology of the crab shell powder shows a predominance of a nail head and cubic-like structure, which is the characteristic of calcite crystals [25,26].

Energy Dispersive X-ray Analysis (EDX), referred to as EDS or EDAX, is used to determine the mineral content of green mussel and crab shell powder. Table 1 shows a summary of the EDX results of green mussel and crab shell powder, with the major components found to be Ca, C, and O. The EDX test results show the presence of Na in green mussel shells, although in small amounts. Meanwhile, in crab shells, Na, Mg, P, and Zr are found in addition to Ca, C, and O elements.

Table 1. The summary of EDX results on the green mussel and crab shells.

Element	Composition (wt.%)	
	Crab Shells	Green Mussel Shells
C	29.44	17.56
O	38.97	53.09
Ca	24.49	28.85
Na	0.38	0.50
Mg	1.4	-
P	3.33	-
Zr	1.99	-
Total	100	100

3.2. Characterization of Green Mussel and Crab Shell Powders after Calcination

In this study, the calcination process was carried out on the powder of the green mussel and crab shells using a Thermolyne Furnace Chamber F6010 at a temperature of 900 °C for 5 h. Here, calcination produces Calcined Green Mussel Shells (CMS) and Calcined Crab Shells (CCS). Figure 5 shows a graphic comparison of the results of XRD testing on CMS and CCS with the dominance of the portlandite crystal phase. Portlandite was observed at 2θ: 18.0123, 34.1015, and 50.7966 (JCPDS Card No. 44-1481). Calcination is generally used to remove organic compounds and impurities in green mussel powder and crab shells. In addition, calcination in green mussel powder and crab shells with a temperature of 900 °C for 5 h to convert the CaCO₃ compound into CaO is given in the reaction equation [27]:

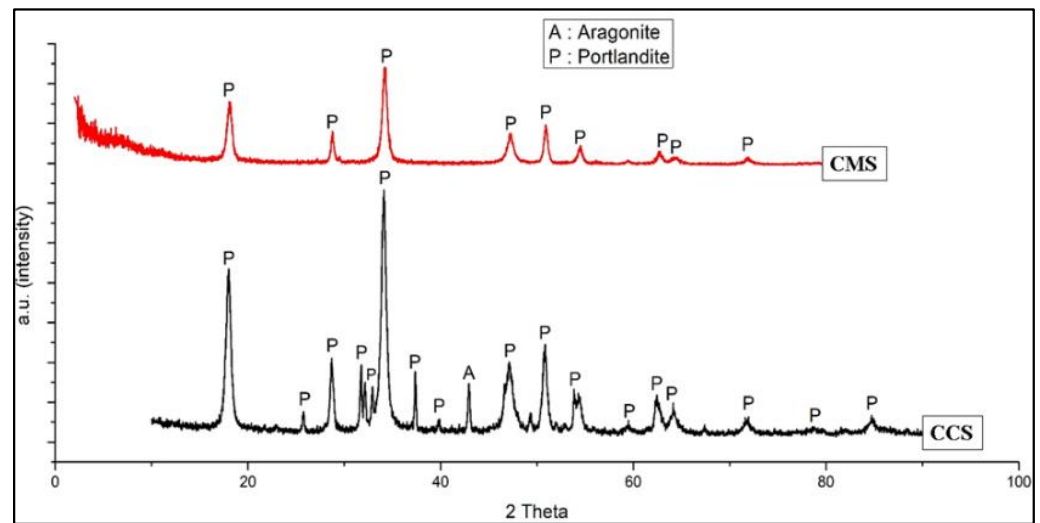
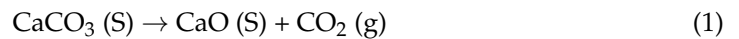
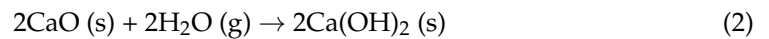


Figure 5. XRD diffraction pattern of CMS and CCS.

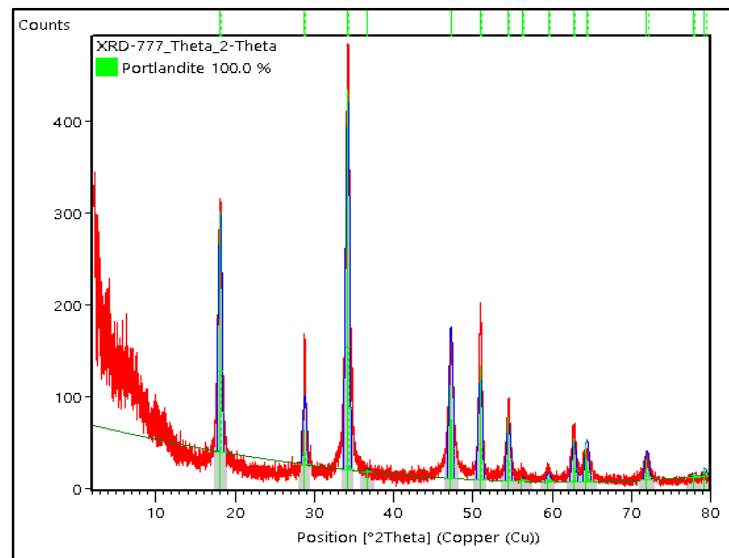
After 5 h, cooling down to room temperature was held by turning off the furnace without opening it (cooling in the furnace). It was done to avoid the possibility of damage to the furnace walls due to the sudden change of temperature. After reaching room temperature, the furnace was opened to collect the green mussel and crab shell powders.

During the cooling process, there was contact between the CaO compound in the green mussel and crab shell powders with air containing water vapor so that hydration could occur, and portlandite or $\text{Ca}(\text{OH})_2$ was formed through the reaction equation [27]:

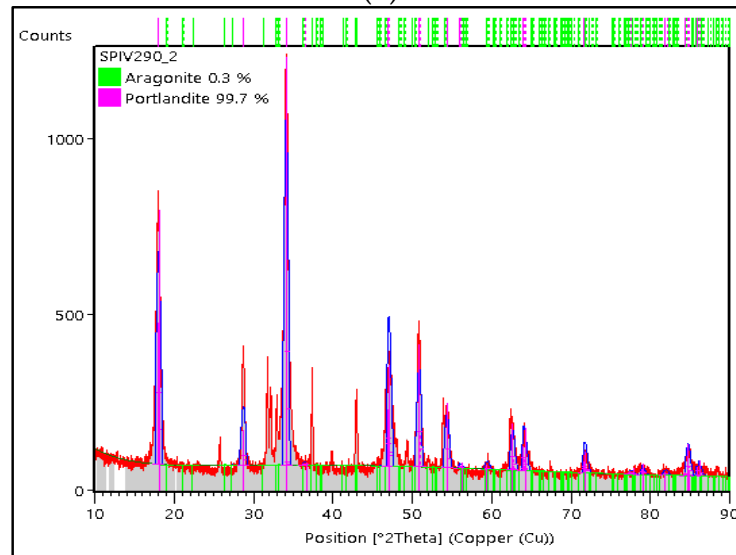


This is what causes the calcite and aragonite crystals in the powder of green mussel and crab shells to transform into calcium hydroxide or portlandite ($\text{Ca}(\text{OH})_2$) after calcination [27,28].

In this study, only a portlandite crystal phase was found in CMS, while in CCS, there was still a small amount of aragonite crystal phase. The weight percentage (%) of the portlandite crystal phase was generated from a Rietveld analysis using High Score Plus software version 3.0e, as shown in Figure 6a,b. In CMS, the portlandite crystal has a weight percentage (%) and crystallite size of 100% and 14 nm, respectively, with the trigonal crystal system. Meanwhile, the portlandite phase on CCS shows a trigonal crystal system with a weight percentage (%) and crystallite size of 99.7% and 12 nm, respectively. Apart from the portlandite phase, aragonite crystals in CCS were also found with a weight percentage (%) of 0.3%. The XRD test results on the CMS and CCS are supported by the SEM test results, as shown in Figure 7a,b. As a result of the study, portlandite crystallized in the shape of imperfect cubic and irregular shapes. The portlandite crystals' morphology in this study is consistent with the literature [29,30].

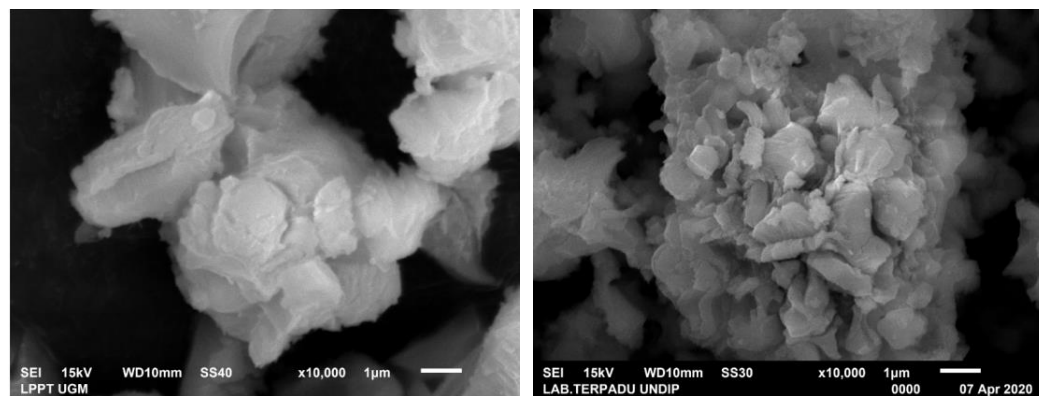


(a)



(b)

Figure 6. X-ray diffraction patterns of (a) CMS and (b) CCS.



(a)

(b)

Figure 7. SEM images of (a) CMS and (b) CCS.

Table 2 shows a summary of the EDX results on CMS and CCS with the major components found being Ca, C, and O. The EDX test results show that the Na element in green mussel shells powder before calcination was not found in CMS. Meanwhile, in CCS, there were still elements of Na, Mg, and P, and Ca, C, and O. After calcination, the Ca content in CMS and CCS was more than the Ca content in the green mussel and crab shell powders. Meanwhile, the C content in CMS and CCS was less than the C content in the green mussel and crab shell powders. This happened because of the decomposition process, where C bound to O to form CO₂ gas and Ca bound to O to form CaO.

Table 2. The summary of EDX results on CMS and CCS.

Element	Composition (wt.%)			
	Green Mussel Shells		Crab Shells	
	Powders	CMS	Powders	CCS
C	17.56	7.13	29.44	7.38
O	53.09	51.21	38.97	47.99
Ca	28.85	41.66	24.49	37.18
Na	0.5	-	0.38	0.58
Mg	-	-	1.4	3.89
P	-	-	3.33	2.98
Zr	-	-	1.99	-
Total	100	100	100	100

3.3. Characterization of Green Mussel and Crab Shell Powders after Precipitation Process

In this study, the Precipitated Calcium Carbonate (PCC) produced from green mussel shells powder was labeled as PMS, whilst the Precipitated Calcium Carbonate (PCC) produced from crab shells powder was labeled as PCS.

Figure 8 shows a comparison graph of the XRD test results on PMS and PCS. The crystalline phases of vaterite, calcite, and aragonite were found in PMS and PCS. Following JCPDS card number 13-0192, the phase of the vaterite crystal in PMS and PCS is denoted by 2 θ : 24.9011, 27.0705, and 32.7760. In addition to that, there were calcite and aragonite crystal phases that correspond to the JCPDS card numbers 05-0586 and 05-0453. In this study, PMS and PCS were dominated by the vaterite crystalline phase, with a few calcite and aragonite crystalline phases.

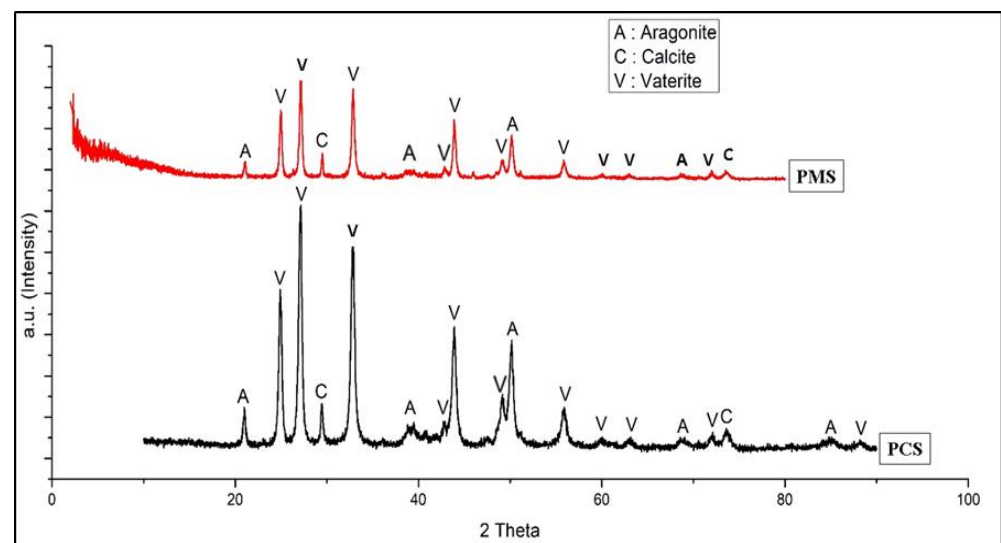
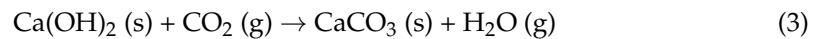


Figure 8. XRD diffraction pattern of PMS and PCS.

In this study, CMS and CCS with portlandite or $\text{Ca}(\text{OH})_2$ as the dominant phase was converted to PMS and PCS, which had CaCO_3 (vaterite) as the predominant crystal phase precipitation process using CO_2 gas. CaCO_3 may be obtained when portlandite ($\text{Ca}(\text{OH})_2$) was exposed to atmospheric carbon dioxide (CO_2). The transformation of portlandite to CaCO_3 is under the equation [30]:



The formation of the vaterite dominant phase in PMS and PCS can occur due to several things, such as the reaction temperature, Ph, and CO_2 flow rate at the time of carbonation [31,32]. In this study, the carbonation process was carried out at a temperature of 30°C , pH 12 and a low flow rate of CO_2 . The dominant vaterite phase was caused by an increase in the concentration of CO_2 gas. That happens because the amount of CO_2 gas added will increase the solubility of CO_2 gas in the solution. The increasing solubility of CO_2 gas in the solution causes an increase in the supersaturation of the solution so that vaterite is formed as the dominant crystalline phase [33].

A comparison of the weight percentage (%) phase of vaterite, calcite, and aragonite crystals on PMS and PCS is shown in Figure 9.

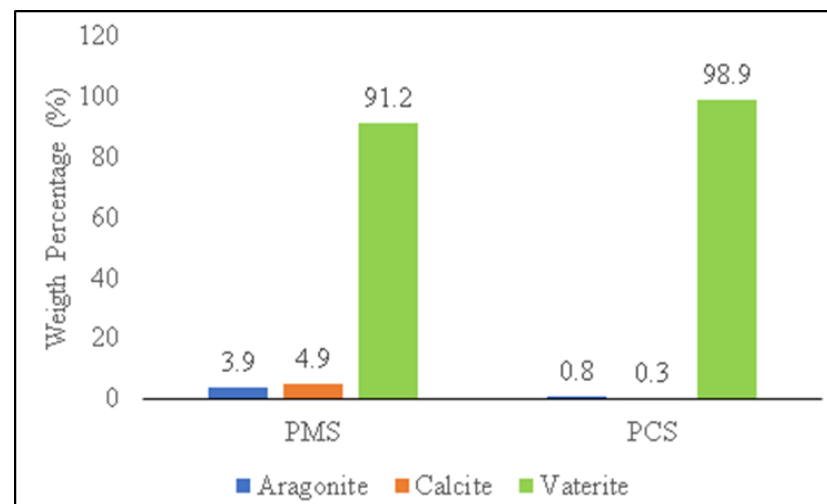
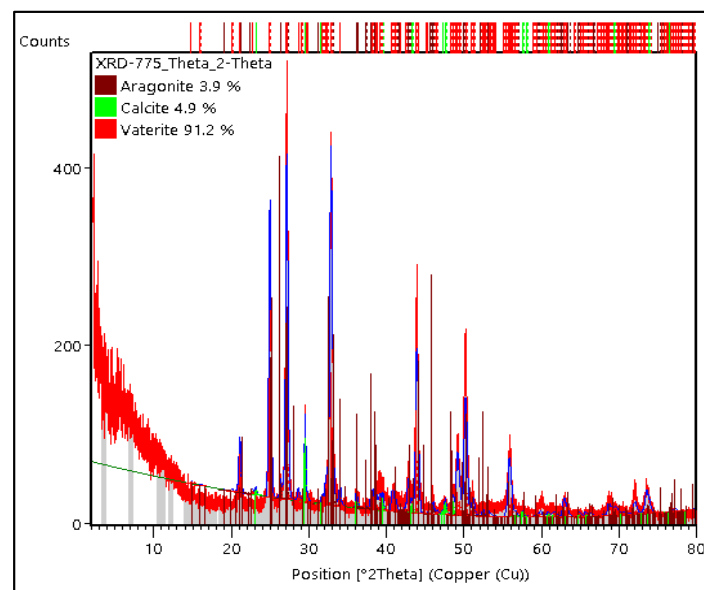


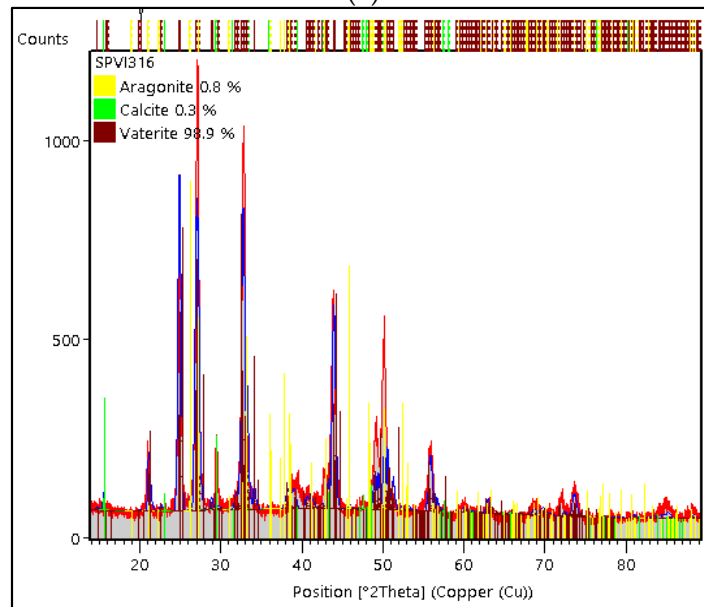
Figure 9. Weight percentage (%) comparison of crystal phase on PMS and PCS.

The weight percentage (%) was generated from Rietveld analysis conducted using High Score Plus software version 3.0e, as shown in Figure 10a,b. In PMS, the vaterite crystal had a weight percentage (%) and crystallite size of 91.2% and 34 nm, respectively, with the monoclinic crystal system. Meanwhile, the weight percentage (%) on calcite and aragonite was 4.9% and 3.9%, respectively. The vaterite phase of PCS shows the monoclinic crystal system with a weight percentage (%) and crystallite size of 98.9% and 21 nm, respectively. Apart from the vaterite phase, PCS also found aragonite and calcite crystals with a weight percentage (%) of 0.8% and 0.3%, respectively.

The test results on PMS and PCS showed the dominance of the vaterite crystal phase. The results of the SEM tests support these results carried out as shown in Figure 11a,b. As a result of the study, vaterite was crystallized in a spherical shape. The vaterite crystals' morphology in this study is consistent with the literature [34,35]. Table 3 summarizes the EDX results on PMS and PCS, and the major components found are Ca, C, and O. After precipitation, PMS and PCS experience a decrease in Ca content due to the addition of CO_2 gas into the solution. This is proved by the increase in the C and O content. EDX testing showed that only Ca, C, and O were found in PMS. Meanwhile, PCS found N elements other than Ca, C, and O. Element N found in PCS was caused by mixing less homogeneous $\text{Ca}(\text{OH})_2$ with 2M HNO_3 , leading to a less perfect reaction of NO_3^- ions.

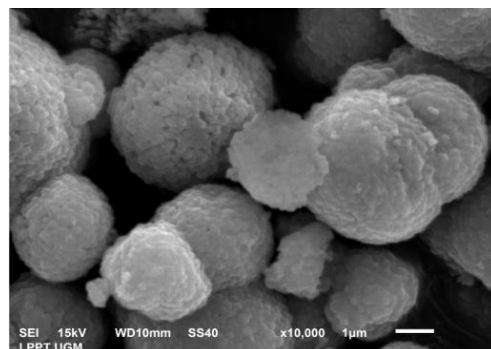


(a)

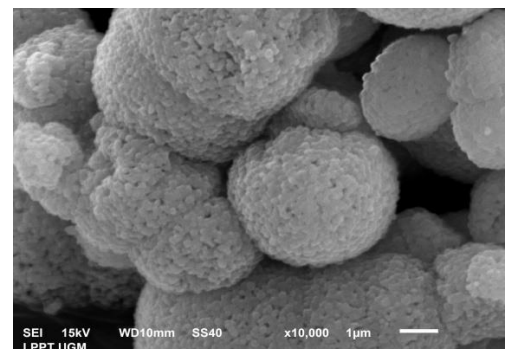


(b)

Figure 10. X-ray diffraction patterns of (a) PMS and (b) PCS.



(a)



(b)

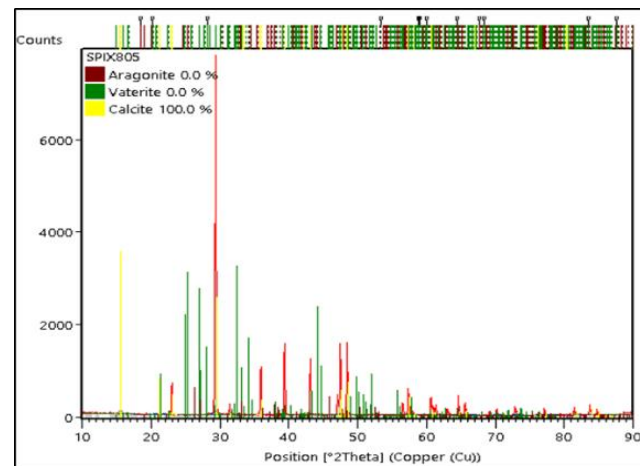
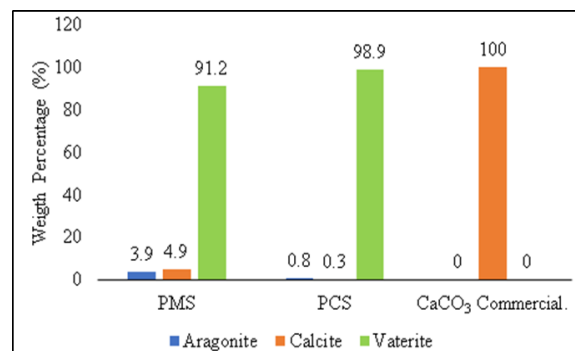
Figure 11. SEM images of (a) PMS and (b) PCS.

Table 3. The summary of EDX results on PMS and PCS.

Element	Composition (wt.%)					
	Green Mussel Shells			Crab Shells		
	Powders	CMS	PMS	Powders	CCS	PCS
C	17.56	7.13	14.11	29.44	7.38	15.43
O	53.09	51.21	52.41	38.97	47.99	54.44
Ca	28.85	41.66	33.48	24.49	37.18	17.56
Na	0.5	-	-	0.38	0.58	-
Mg	-	-	-	1.4	3.89	-
P	-	-	-	3.33	2.98	-
Zr	-	-	-	1.99	-	-
Total	100	100	100	100	100	100

3.4. The Comparison of the Characterization of PMS, PCS, and Commercial CaCO_3

The XRD test results' analysis on commercial CaCO_3 were carried out with Rietveld analysis using High Score Plus software version 3.0e to determine the crystal phase formed, weight percentage (%), and crystallite size, as shown in Figure 12. In commercial CaCO_3 , there was only a calcite phase as a single phase with a trigonal crystal system. The weight percentage (%) and crystallite size of calcite on commercial CaCO_3 were 100% and 15 nm, respectively. The crystallite size for commercial CaCO_3 was 15 nm, while the crystallite size for PMS and PCS were 34 nm and 21 nm, respectively. A comparison of the weight percentage (%) for each crystal phase found in PMS, PCS, and commercial CaCO_3 is shown in Figure 13. In commercial CaCO_3 , there is only calcite as a single phase. Whereas in PMS and PCS, vaterite is the dominant crystalline phase.

**Figure 12.** X-ray Diffraction Patterns of Commercial CaCO_3 .**Figure 13.** Weight Percentage Comparison (%) of Crystal Phase on PMS, PCS, and Commercial CaCO_3 .

In this study, after the carbonation process of the calcined powder was produced from green mussel and crab shells, vaterite was the dominant crystalline phase in the calcium carbonate polymorph. Similar findings were reported by Prihanto et al. (2022). A quantitative XRD Rietveld examination of PCC products generated from green mussel shells revealed the presence of vaterite (55.20 wt %) and calcite (44.40 wt %) minerals following the carbonation of the calcined powder product [36]. According to Ismail et al. (2021), no polymorphic difference was noticed between the PCC product and the CO₂ stream in contact with the reaction solution. Importantly, PCC-800 and PCC-900 products include a high concentration of vaterite, a promising biomaterial for use in drug delivery systems [19].

The crystalline phase of calcium carbonate is generally in the form of calcite, aragonite, and vaterite. The different morphological forms are due to different synthesis conditions [37,38]. Calcite has stable structures, mechanical properties, and thermodynamic properties, so it is widely used in biomedical applications [39]. Aragonite is formed in the orthorhombic system and is biocompatible. Aragonite can be broken down, combined, and it can also replace bone. Aragonite is denser than calcite and has also been used for biomedical applications [40,41]. Vaterite has low stability and belongs to the hexagonal crystal system. In contact with water, vaterite can slowly dissolve and recrystallize to a stable form [42]. Due to its nontoxicity, good biocompatibility and affinity, low cost, and ease of large-scale production, vaterite can be used as an ideal nominee for biomedical applications [35,42]. The XRD results on commercial CaCO₃ are supported by the SEM test results shown in Figure 14. Commercial CaCO₃ has a morphology with a cube-like shape, which is characteristic of calcite [37]. Meanwhile, PMS and PCS have spherical morphology, which is characteristic of vaterite crystals. The results of this study are the same as the research conducted by Hamester et al. (2012) [43].

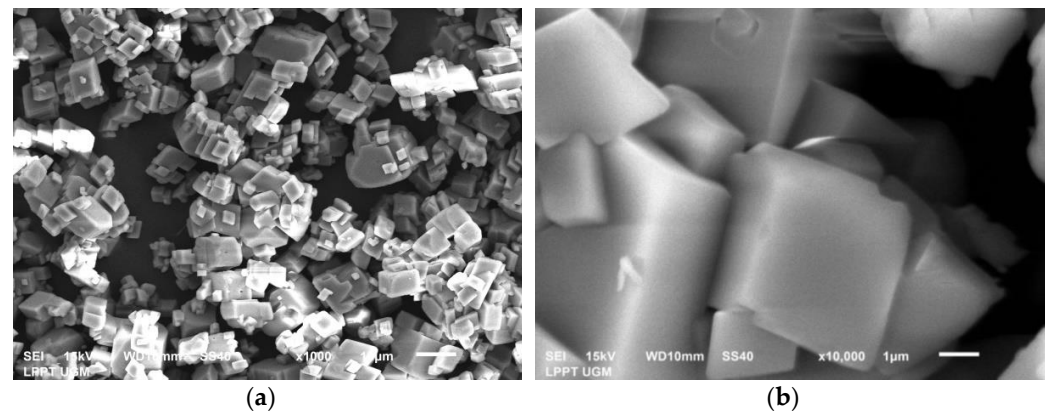


Figure 14. SEM images with different magnifications of (a) 1000 and (b) 10,000 times of commercial CaCO₃.

The EDX test results show that PMS and commercial CaCO₃ only contain Ca, C, and O. Meanwhile, PCS found the presence of N elements besides Ca, C, and O. The results of the research conducted by [44] stated that the chemical composition of commercial CaCO₃ (calcite) consists of only Ca, C, and O. The common elements such as Ca, C, and O were present in the CaCO₃ derived from green mussel shells (PMS), indicating the success of the precipitation method [45]. The comparison of the chemical composition of PMS, PCS, and commercial CaCO₃ is shown in Figure 15. In this study, the Ca content in commercial CaCO₃ was higher than the Ca content in PMS and PCS. While the C and O content in commercial CaCO₃ was lower than the C and O content in PMS and PCS. In this study, the chemical composition of PMS was better than the chemical composition of PCS. Moreover, the chemical composition of PMS was almost the same as the chemical composition of commercial CaCO₃. In addition, in PMS, there were no impurities.

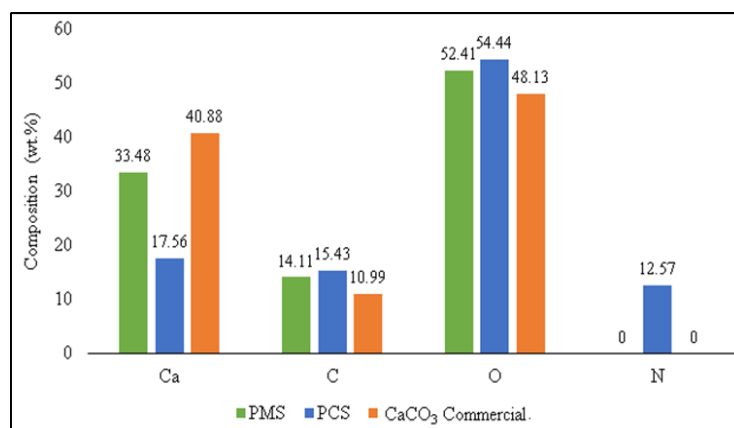


Figure 15. Chemical Composition Comparison of PMS, PCS, and Commercial CaCO₃.

A similar result was stated by Ismail et al. (2021). The EDX analysis revealed that PCC samples derived from green mussel shells (PCC-800 and PCC-900) included primarily Ca, C, and O. Introducing a stream of CO₂ into the solution caused a decrease in the Ca concentration of PCC samples. Conversely, the carbonization process raises the C and O concentration [19]. Prihanto et al. (2022) discovered differences showing that in addition to Ca, C, and O, PCC derived from green mussel shells contained Zn and Cu. Based on the EDX analysis, secondary reactions involving the formation of solid solutions correlating to the existence of Cu and Zn may also exist, especially along the adsorption–precipitation boundary [36].

4. Conclusions

The use of green mussel and crab shells after industrial and consumption activities has many benefits. It has the potential to be applied in various fields, including in the field of biomaterials. This research shows that the calcination and precipitation processes significantly affect the chemical composition, crystal phase, crystal size, and crystal system of the CaCO₃ obtained. The crystalline phases of aragonite and calcite in green mussel and crab shell powders were converted to Ca(OH)₂ or portlandite by calcination. In addition, calcination can remove organic compounds and reduce the impurity content in green mussel powder and crab shells. The chemical composition of PMS and commercial CaCO₃ shows that they existed only as Ca, C, and O. In contrast, in PCS, it was found that the element N is an impurity in addition to Ca, C, and O. The results of this study show that PMS can be used as a candidate for biomaterials because the chemical composition in PMS is almost the same as the chemical composition in commercial CaCO₃, where no impurities were found. In addition, the dominance of the vaterite crystal phase in PMS is a distinct advantage for biomaterial applications because it has nontoxicity, good biocompatibility and affinity, a low cost, and ease of large-scale production.

The crystallite size produced in PMS is more prominent than commercial CaCO₃. The crystallite size of vaterite in PMS is 34 nm, while the crystallite size of calcite in commercial CaCO₃ is 15 nm.

Author Contributions: R.I.: Writing—Original draft, Investigation; T.C.: Project administration, Funding Acquisition; W.L.S.: Writing—review and editing, funding acquisition; D.F.F.: Investigation, formal analysis; J.P.S.: Supervision, formal analysis; A.P.B.: Methodology, Resource; F.W.N.: Visualization, validation; R.C.M.: Investigation; R.J.: Writing—review & editing, visualization; N.A.E.: Writing—review & editing, visualization. All authors have read and agreed to the published version of the manuscript.

Funding: This study was funded by the Ministry of Research and Technology/National Research and Innovation Agency of the Republic of Indonesia, Directorate of Research and Community Services (DRPM) with Grant-No: 225-106/UN7.6.1/PP/2021 and INTI International University.

Institutional Review Board Statement: Not applicable.

Informed Consent Statement: Not applicable.

Data Availability Statement: Data are contained within the article.

Acknowledgments: The authors would like to express their gratitude to the Ministry of Research and Technology/National Research and Innovation Agency of the Republic of Indonesia, Directorate of Research and Community Services (DRPM), for the PDUPT Research Grant in the year 2021. The material characterization partially supported by the research fund from the Faculty of Engineering, Diponegoro University in Strategic Research Scheme, 2020 and INTI International University.

Conflicts of Interest: The authors declare no conflict of interest.

References

1. Venugopal, V.; Gopakumar, K. Shellfish: Nutritive Value, Health Benefits, and Consumer Safety. *Compr. Rev. Food Sci. Food Saf.* **2017**, *16*, 1219–1242. [[CrossRef](#)] [[PubMed](#)]
2. Bps.go.id Fishery. Available online: <https://jateng.bps.go.id/subject/56/perikanan.html#subjekViewTab3> (accessed on 2 July 2021).
3. Faqir, A. Al Tembus Hingga AS, Ekspor Rajungan Indonesia 2019 Cetak Rp5,3 Triliun | Merdeka.com. Available online: <https://www.merdeka.com/uang/tembus-hingga-as-ekspor-rajungan-indonesia-2019-cetak-rp-53-triliun.html> (accessed on 2 July 2021).
4. Fitriyana, D.F.; Ismail, R.; Santosa, Y.I.; Nugroho, S.; Hakim, A.J.; Syahreza Al Mulqi, M. Hydroxyapatite Synthesis from Clam Shell Using Hydrothermal Method: A Review. In Proceedings of the 2019 International Biomedical Instrumentation and Technology Conference, Special Region of Yogyakarta, Indonesia, 23–24 October 2019; pp. 7–11.
5. Raya, I.; Mayasari, E.; Yahya, A.; Syahrul, M.; Latunra, A.I. Synthesis and Characterizations of Calcium Hydroxyapatite Derived from Crabs Shells (*Portunus Pelagicus*) and Its Potency in Safeguard against Dental Demineralizations. *Int. J. Biomater.* **2015**, *2015*, 1–8. [[CrossRef](#)] [[PubMed](#)]
6. Sali, S.S. *Natural Calcium Carbonate for Biomedical Applications*; Indian Institute Of Technology–Bombay (IITB): Mumbai, India, 2015.
7. Yang, H.; Yan, N. Transformation of Seafood Wastes into Chemicals and Materials. In *Encyclopedia of Sustainability Science and Technology*; Springer: New York, NY, USA, 2018; pp. 1–23.
8. Costa, L.M.M.; de Olyveira, G.M.; Salomão, R. Precipitated Calcium Carbonate Nano-Microparticles: Applications in Drug Delivery. *Adv. Tissue Eng. Regen. Med. Open Access* **2017**, *3*, 1–6. [[CrossRef](#)]
9. Bamigboye, G.; Enabulele, D.; Odetoan, A.O.; Kareem, M.A.; Nworgu, A.; Basse, D.; Bamigboye, G.O.; Shukla, S.K. Mechanical and Durability Assessment of Concrete Containing Seashells: A Review Mechanical and Durability Assessment of Concrete Containing Seashells: A Review Public Interest Statement. *Cogent Eng.* **2021**, *8*, 1883830. [[CrossRef](#)]
10. Fitriyana, D.F.; Nugraha, F.W.; Laroybafih, M.B.; Ismail, R.; Bayuseno, A.P.; Muhamadin, R.C.; Ramadan, M.B.; Qudus, A.R.A.; Siregar, J.P. The Effect of Hydroxyapatite Concentration on the Mechanical Properties and Degradation Rate of Biocomposite for Biomedical Applications. *IOP Conf. Ser. Earth Environ. Sci.* **2022**, *969*, 12045. [[CrossRef](#)]
11. Coringa, R.; de Sousa, E.M.; Botelho, J.N.; Diniz, R.S.; de Sá, J.C.; Nogueira da Cruz, M.C.F.; Paschoal, M.A.B.; Gonçalves, L.M. Bone Substitute Made from a Brazilian Oyster Shell Functions as a Fast Stimulator for Bone-Forming Cells in an Animal Model. *PLoS ONE* **2018**, *13*, e0198697. [[CrossRef](#)]
12. Oktawati, S.; Mappangara, S.; Chandra, H.; Achmad, H.; Raoda, S.; Ramadhan, J.; Dwipa, G.; Yudin, M. Effectiveness Nacre Pearl Shell (*Pinctada Maxima*) as Bone Graft for Periodontal Bone Remodeling. *Ann. Rom. Soc. Cell Biol.* **2021**, *25*, 8663–8678.
13. Musa, B.; Raya, I.; Natsir, H. Synthesis and Characterizations of Hydroxyapatite Derived Blood Clam Shells (*Anadara Granosa*) and Its Potency to Dental Remineralizations. *Int. J. Appl. Chem.* **2016**, *12*, 527–538.
14. Albadr, R.M.; Halfi, S.A.; Ziadan, K.M. The Effectiveness of Oyster Filler on the Physical and Mechanical Properties of Novel Dental Restorative Composite. *AIP Conf. Proc.* **2020**, *2290*, 50001.
15. Fu, W.; Mohd Noor, M.H.; Yusof, L.M.; Ibrahim, T.A.T.; Keong, Y.S.; Jaji, A.Z.; Zakaria, M.Z.A.B. In Vitro Evaluation of a Novel PH Sensitive Drug Delivery System Based Cockle Shell-Derived Aragonite Nanoparticles against Osteosarcoma. *J. Exp. Nanosci.* **2017**, *12*, 166–187. [[CrossRef](#)]
16. Saidykhan, L.; Bakar, M.Z.B.A.; Rukayadi, Y.; Kura, A.U.; Latifah, S.Y. Development of Nanoantibiotic Delivery System Using Cockle Shell-Derived Aragonite Nanoparticles for Treatment of Osteomyelitis. *Int. J. Nanomed.* **2016**, *11*, 661–673. [[CrossRef](#)]
17. Choi, A.H.; Cazalbou, S.; Ben-Nissan, B. Biomimetics and Marine Materials in Drug Delivery and Tissue Engineering. In *Handbook of Bioceramics and Biocomposites*; Springer: Berlin/Heidelberg, Germany, 2016; pp. 521–544. ISBN 9783319124605.
18. Zhao, R.; Yang, R.; Cooper, P.R.; Khurshid, Z.; Shavandi, A.; Ratnayake, J. Bone Grafts and Substitutes in Dentistry: A Review of Current Trends and Developments. *Molecules* **2021**, *26*, 3007. [[CrossRef](#)] [[PubMed](#)]
19. Ismail, R.; Fitriyana, D.F.; Santosa, Y.I.; Nugroho, S.; Hakim, A.J.; Al Mulqi, M.S.; Jamari, J.; Bayuseno, A.P. The Potential Use of Green Mussel (*Perna Viridis*) Shells for Synthetic Calcium Carbonate Polymorphs in Biomaterials. *J. Cryst. Growth* **2021**, *572*, 126282. [[CrossRef](#)]

20. Fitriyana, D.F.; Caesarendra, W.; Nugroho, S.; Haryadi, G.D.; Herawan, M.A.; Rizal, M.; Ismail, R. The Effect of Compressed Air Pressure and Stand-off Distance on the Twin Wire Arc Spray (TWAS) Coating for Pump Impeller from AISI 304 Stainless Steel. *Springer Proc. Phys.* **2020**, *242*, 119–130. [[CrossRef](#)]
21. Fitriyana, D.F.; Suhaimi, H.; Sulardjaka; Noferi, R.; Caesarendra, W. Synthesis of Na-P Zeolite from Geothermal Sludge. *Springer Proc. Phys.* **2020**, *242*, 51–59. [[CrossRef](#)]
22. Fitriyana, D.F.; Anis, S.; Rachman, A.; Qudus, A.; Aufa, M.; Lakuy, N.; Ismail, R.; Nugroho, S.; Haryadi, G.D.; Bayuseno, A.P. The Effect of Post-Heat Treatment on The Mechanical Properties of FeCrBMnSi Coatings Prepared by Twin Wire Arc Spraying (TWAS) Method on Pump Impeller From 304 Stainless Steel. *J. Adv. Res. Fluid Mech. Therm. Sci.* **2022**, *2*, 138–147. [[CrossRef](#)]
23. Huang, Z.Q.; Zhang, G.S.; Tan, Y. Gelatinous Siphon Sheath Templates the Starfruit-Shaped Aragonite Aggregate Growth. *J. Nanomater.* **2019**, *2019*, 1–9. [[CrossRef](#)]
24. Ramakrishna, C.; Thenepalli, T.; Ahn, J.W. A Brief Review of Aragonite Precipitated Calcium Carbonate (PCC) Synthesis Methods and Its Applications. *Korean Chem. Eng. Res.* **2017**, *55*, 443–455. [[CrossRef](#)]
25. Widayastuti, S.; Intan Ayu Kusuma, P. Synthesis and Characterization of CaCO₃ (Calcite) Nano Particles from Cockle Shells (*Anadara Granosa Linn*) by Precipitation Method. *AIP Conf. Proc.* **2017**, *1855*, 030018. [[CrossRef](#)]
26. Oral, Ç.M.; Ercan, B. Influence of PH on Morphology, Size and Polymorph of Room Temperature Synthesized Calcium Carbonate Particles. *Powder Technol.* **2018**, *339*, 781–788. [[CrossRef](#)]
27. Loy, C.W.; Matori, K.A.; Lim, W.F.; Schmid, S.; Zainuddin, N.; Wahab, Z.A.; Alassan, Z.N.; Zaid, M.H.M. Effects of Calcination on the Crystallography and Nonbiogenic Aragonite Formation of Ark Clam Shell under Ambient Condition. *Adv. Mater. Sci. Eng.* **2016**, *2016*, 2914368. [[CrossRef](#)]
28. Jimoh, O.A.; Ariffin, K.S.; Hussin, H.B.; Temitope, A.E. Synthesis of Precipitated Calcium Carbonate: A Review. *Carbonates Evaporites* **2018**, *33*, 331–346. [[CrossRef](#)]
29. Yakymchko, Y.; Sanytsky, M.; Chekanskyi, B. Research of Alteration of Portlandite Crystals Habit as a Factor of Structure Formation Control for Lime-Containing Binders. *Eureka Phys. Eng.* **2016**, *6*, 19–28. [[CrossRef](#)]
30. Franus, W.; Panek, R.; Wdowin, M. Sem Investigation of Microstructures in Hydration Products of Portland Cement. In *2nd International Multidisciplinary Microscopy and Microanalysis Congress*; Springer: Cham, Switzerland, 2015; Volume 164, pp. 105–112.
31. Wardhani, S.; Prasetya, F.; Khunur, M.M.; Purwonugroho, D.; Prananto, Y.P. Effect of CO₂ Flow Rate and Carbonation Temperature in the Synthesis of Crystalline Precipitated Calcium Carbonate (PCC) from Limestone. *Indones. J. Chem.* **2018**, *18*, 573–579. [[CrossRef](#)]
32. Gomez-Villalba, L.S.; López-Arce, P.; Alvarez De Buergo, M.; Fort, R. Atomic Defects and Their Relationship to Aragonite-Calcite Transformation in Portlandite Nanocrystal Carbonation. *Cryst. Growth Des.* **2012**, *12*, 4844–4852. [[CrossRef](#)]
33. Ismail, R.; Laroybafih, M.B.; Fitriyana, D.F.; Nugroho, S.; Santoso, Y.I.; Hakim, A.J.; Mulqi, M.S.A.; Priharyoto, A. The Effect of Hydrothermal Holding Time on The Characterization of Hydroxyapatite Synthesized from Green Mussel Shells. *J. Adv. Res. Fluid Mech. Therm. Sci.* **2021**, *80*, 84–93. [[CrossRef](#)]
34. Trushina, D.B.; Bukreeva, T.V.; Kovalchuk, M.V.; Antipina, M.N. CaCO₃ Vaterite Microparticles for Biomedical and Personal Care Applications. *Mater. Sci. Eng. C* **2014**, *45*, 644–658. [[CrossRef](#)]
35. Konopacka-Lyskawa, D.; Kościelska, B.; Łapiński, M. Precipitation of Spherical Vaterite Particles via Carbonation Route in the Bubble Column and the Gas-Lift Reactor. *JOM* **2019**, *71*, 1041–1048. [[CrossRef](#)]
36. Prihanto, A.; Muryanto, S.; Ismail, R.; Jamari, J.; Bayuseno, A.P. Practical Insights into the Recycling of Green Mussel Shells (*Perna Viridis*) for the Production of Precipitated Calcium Carbonate. *Environ. Technol.* **2022**, 1–11. [[CrossRef](#)]
37. Hu, H.; Zhang, Y.; Zhang, X.; Deb, H.; Yao, J. Phase Selection of Calcium Carbonate Crystals under the Induction of Lignin Monomer Model Compounds. *CrystEngComm* **2020**, *22*, 2454–2461. [[CrossRef](#)]
38. Kamitakahara, M.; Nagamori, T.; Yokoi, T.; Ioku, K. Carbonate-Containing Hydroxyapatite Synthesized by the Hydrothermal Treatment of Different Calcium Carbonates in a Phosphate-Containing Solution. *J. Asian Ceram. Soc.* **2015**, *3*, 287–291. [[CrossRef](#)]
39. Mayorga, I.C.; Astilleros, J.M.; Fernández-Díaz, L. Precipitation of CaCO₃ Polymorphs from Aqueous Solutions: The Role of Ph and Sulphate Groups. *Minerals* **2019**, *9*, 178. [[CrossRef](#)]
40. Mailafiya, M.M.; Abubakar, K.; Danmaigoro, A.; Chiroma, S.M.; Rahim, E.B.A.; Moklas, M.A.M.; Zakaria, Z.A.B. Cockle Shell-Derived Calcium Carbonate (Aragonite) Nanoparticles: A Dynamite to Nanomedicine. *Appl. Sci.* **2019**, *9*, 2897. [[CrossRef](#)]
41. Habte, L.; Khan, M.D.; Shiferaw, N.; Farooq, A.; Lee, M.; Jung, S.; Ahn, J.W. Synthesis, Characterization and Mechanism Study of Green Aragonite Crystals Fromwaste Biomaterials as Calcium Supplement. *Sustainability* **2020**, *12*, 5062. [[CrossRef](#)]
42. Konopacka-Lyskawa, D. Synthesis Methods and Favorable Conditions for Spherical Vaterite Precipitation: A Review. *Crystals* **2019**, *9*, 223. [[CrossRef](#)]
43. Hamester, M.R.R.; Balzer, P.S.; Becker, D. Characterization of Calcium Carbonate Obtained from Oyster and Mussel Shells and Incorporation in Polypropylene. *Mater. Res.* **2012**, *15*, 204–208. [[CrossRef](#)]
44. Awe, O.W.; Minh, D.P.; Lyczko, N.; Nzihou, A.; Zhao, Y. Laboratory-Scale Investigation of the Removal of Hydrogen Sulfide from Biogas and Air Using Industrial Waste-Based Sorbents. *J. Environ. Chem. Eng.* **2017**, *5*, 1809–1820. [[CrossRef](#)]
45. Hussein, A.I.; Ab-Ghani, Z.; Che Mat, A.N.; Ab Ghani, N.A.; Husein, A.; Ab Rahman, I. Synthesis and Characterization of Spherical Calcium Carbonate Nanoparticles Derived from Cockle Shells. *Appl. Sci.* **2020**, *10*, 7170. [[CrossRef](#)]